# Journal of Materials Chemistry C

Accepted Manuscript


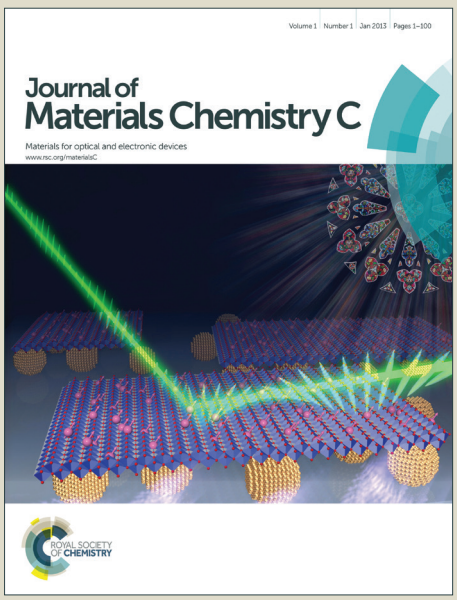





ROYAL SOCIETY OF CHEMISTRY

www.rsc.org/materialsC

Cite this: DOI: 10.1039/c0xx00000x

www.rsc.org/xxxxxx

ARTICLE TYPE

# From Non-Detectable to Decent: Replacement of Oxygen with Sulfur in Naphthalene Diimide Boosts Electron Transport in Organic Thin-Film Transistors (OTFT)

**Wangqiao Chen,[a,b‡] Jing Zhang,[a‡] Guankui Long,[a] Yi Liu,[c] Qichun Zhang[*a,b,d]**

***Received (in XXX, XXX) Xth XXXXXXXXX 20XX, Accepted Xth XXXXXXXXX 20XX***
**DOI: 10.1039/b000000x**

Enhancing the electron mobility of organic conjugated materials without tedious modification or synthesis is highly desirable and practical. In this research, we demonstrated that the electron mobility of naphthalene diimide (NDI) in thin film transistors (TFTs) under ambient conditions can be dramatically enhanced through a simple step reaction by replacing oxygen atoms with sulfur atoms. The electron mobilities of as-prepared compounds range from non-detectable (parent **NDI**), to $3.0\times10^{-4}$ $cm^2$ $V^{-1}$ $s^{-1}$ (**NDI-1S**), $3.0\times10^{-3}$ $cm^2$ $V^{-1}$ $s^{-1}$ (**NDI-3S**), $3.7\times10^{-3}$ $cm^2$ $V^{-1}$ $s^{-1}$ (**NDI-2S-cis**), and 0.01 $cm^2$ $V^{-1}$ $s^{-1}$ (**NDI-2S-trans**) with on/off ratio as high as $4\times10^5$. Our primary result suggests that thionation could be a promising method to tune the band position and bandgap of organic semiconductors for high performance TFTs.

## Introduction

Organic semiconducting materials have been strongly investigated in many organic electronic devices including organic field-effect transistors[1-5], sensors,[6-11] and photovoltaics[12-14] due to their charming advantages such as solution processing, large-area manufacture, and easy chemical functionalization. Although a large number of π-conjugated semiconductors have been designed and prepared for applications in organic electronics, how to realize high performance organic electronic devices with reasonable stability and repeatability through simple modification or synthesis is still a big challenge. At present, comparing with p-type organic semiconductors, the research on n-type organic materials is relatively slow. One well-known strategy to achieve n-type material with ideal mobility and ambient stability is to design and obtain novel molecule with suitable LUMO energy and ideal molecule packing for effective charge (electron) transport.[15-18] It has been widely demonstrated that the electron affinity and the air stability of the OFET device will increase simultaneously by introducing electron-withdrawing groups, such as cyano (–CN),[18] chlorine (–Cl),[20] or perfluoroalkyl (–$CF_2$–)[21-22] on the π-conjugated backbone or the substituted alkyl chain. Another approach is to extend the π–conjugated core to achieve graphene-like oligomers with rigidly and almost planar superstructures, which could lead to excellent electron transport characteristics.[23-26] Unfortunately, these approaches generally require multi-step synthesis. Thus, searching a simple and convenient method to develop novel molecules for high-performance n-type OFET is still highly desirable.

Among the current n-type small molecule systems such as naphthalene diimides (NDIs), Perylene diimides (PDIs),[27-28] quinoidal oligothiophenes (QOTs),[29-32] isoindigo[33-44] and fullerenes,[35-37] NDI has been demonstrated to be a promising candidate with various mobility due to the molecule diversity.[38] Meanwhile, introducing sulfur atoms into acene frameworks have been proven to be a general strategy to obtain high charge transport mobility.[39-42] Thus, replacing O with S in NDI system was supposed to be a good strategy to address the issues of mobility and stability because (1) S…..S interaction could enhance the stability of molecular arrangement in space; (2) The absorption and Lowest Unoccupied Molecular Orbital (LUMO) energy can be easily tuned by controlling the number of sulfur atoms; and (3) Thionation can be completed in one step reaction by using Lawesson's reagent (LR). In this research, four compounds 2,7-bis(2-ethylhexyl)-8-thioxo-7,8-dihydrobenzo[lmn][3,8]-phenanthroline-1,3,6(2H)-trione (**NDI-1S**), 2,7-bis(2-ethylhexyl)-3,6-dithioxo-2,3,6,7-tetrahydrobenzo-[lmn][3,8]phenanthroline-1,8-dione (**NDI-2S-cis**), 2,7-bis(2-ethylhexyl)-3,8-dithioxo-2,3,7,8-tetrahydrobenzo-[lmn][3,8]phenanthroline-1,6-dione (**NDI-2S-trans**), and 2,7-bis(2-ethylhexyl)-3,6,8-trithioxo-2,3,7,8-tetrahydrobenzo-[lmn][3,8]phenanthrolin-1(6H)-one (**NDI-3S**) have been synthesized and our studies indicate that more sulfur atoms will result in more red-shift absorption as well as lower LUMO and energy gap. The mobilities of all these materials have been investigated in air and **NDI-2S-trans** showed best mobility of 0.01 $cm^2$ $V^{-1}$ $s^{-1}$ while controlled NDI shows almost no field-effect under ambient condition.

## Experimental section

### Synthesis of NDI-1S, NDI-2S-trans and NDI-2S-cis

A solution of lawesson's reagent (485 mg, 1.2 mmol, 2.0 eq. to

**NDI**) and **NDI** (0.294 mg, 0.6 mmol, 1.0 eq.) in xylene (30 mL) was heated at 140 °C for 2 h under argon. The resulting brown solution was cooled to room temperature and concentrated in vacuum to give a crude mixture of unreacted **NDI**, **NDI-1S, NDI-2S-trans and NDI-2S-cis**. Separation by column chromatography (Hexane/$CH_2CH_2$= 1:1 to 1: 2) gave **NDI-1S, NDI-2S-trans and NDI-2S-cis** in the following yields.

**2,7-bis(2-ethylhexyl)-8-thioxo-7,8-dihydrobenzo[lmn][3,8]-phenanthroline-1,3,6(2H)-trione (NDI-1S):** Green yellow solid, 101mg, Yield: 33%; mp: 175 °C (DSC). $^1$H NMR (300 MHz, $CDCl_3$) δ 9.04 (d, *J* = 9.0 Hz, 1H), 8.75-8.69 (m, 2H), 8.62 (d, *J* = 1.2 Hz, 1H), 4.78-4.65 (m, 2H), 4.19-4.07 (m, 2H), 2.18-2.14 (m, 1H), 1.97-1.91 (m, 1H), 1.40-1.27 (m, 16H), 0.96-0.83 (m, 12H). $^{13}$C NMR (75 MHz, CDCl3) δ 193.5, 163.5, 160.8, 136.0, 131.5, 130.9, 130.5, 130.1, 126.8, 126.6, 126.2, 125.2, 125.0, 50.8, 44.6, 37.9, 36.9, 31.6, 30.7, 28.6, 24.0, 23.0, 22.6, 14.0, 10.7, 10.6. HRMS: calculated for $C_{30}H_{38}N_2O_3S$ + $Na^+$, 529.2501; found: 529.2498 (M+)

**2,7-bis(2-ethylhexyl)-3,8-dithioxo-2,3,7,8-tetrahydrobenzo-[lmn][3,8]phenanthroline-1,6-dione (NDI-2S-trans):** Brown solid, 12 mg, Yield: 4%. mp: 182 °C (DSC); $^1$H NMR (300 MHz, $CDCl_3$) δ 9.04 (d, *J* = 9.0 Hz, 2H), 8.63 (d, *J* = 9.0 Hz, 2H), 4.79-4.66 (m, 4H), 2.21-2.13 (m, 2H), 1.41-1.27 (m, 16H), 0.89-0.83 (m, 12H). $^{13}$C NMR (75 MHz, $CDCl_3$) 193.6, 161.1, 136.0, 131.0, 129.6, 125.3, 125.0, 50.8, 36.9, 30.7, 28.6, 24.0, 23.1, 14.0, 10.7; HRMS: calculated for $C_{30}H_{38}N_2O_2S_2$ + $H^+$, 523.2453; found: 523.2437 (M+)

**2,7-bis(2-ethylhexyl)-3,6-dithioxo-2,3,6,7-tetrahydrobenzo-[lmn][3,8]phenanthroline-1,8-dione (NDI-2S-cis)**: Brown solid, 22 mg, Yield: 7%; m.p: 182 °C (DSC); $^1$H NMR (300 MHz, $CDCl_3$) δ 8.93 (s, 2H), 8.72 (s, 2H), 4.78-4.66 (m, 4H), 2.22-2.11 (m, 2H), 1.38-1.26 (m, 16H), 0.94-0.82 (m, 12H); $^{13}$C NMR (100 MHz, $CDCl_3$) 193.6, 161.1, 135.5, 131.5, 128.8, 126.3, 125.0, 50.8, 37.0, 30.7, 28.6, 24.0, 23.0, 14.0, 10.7; HRMS: calculated for $C_{30}H_{38}N_2O_2S_2$ + $H^+$, 523.2453; found: 523.2459 (M+)

**Synthesis of NDI-3S**

A solution of lawesson's reagent (2.0 g, 4.95 mmol, 5.0 eq. to **NDI**) and **NDI** (0.294 mg, 0.6 mmol, 1.0 eq.) in xylene (30 mL) was heated at 140 °C for 24 h under argon. The resulting brown solution was cooled to room temperature and concentrated in vaccum to give a crude mixture of **NDI-3S, NDI-2S-trans and NDI-2S-cis**. Separation by column chromatography (Hexane/$CH_2CH_2$=1:1 to 1: 2) gave **NDI-2S-trans** (11% yield), **NDI-2S-cis** (9.2%, yield) and **NDI-3S.**

**2,7-bis(2-ethylhexyl)-3,6,8-trithioxo-2,3,7,8-tetrahydrobenzo-[lmn][3,8]phenanthrolin-1(6H)-one (NDI-3S):** red solid, 25 mg, Yield: 4.6%, m.p: 181 °C (DSC); $^1$H NMR (300 MHz, $CDCl_3$) δ 8.90-8.87 (m, 2H), 8.77 (d, *J* = 8.4 Hz, 1H), 8.57 (d, *J* = 8.1 Hz, 1H), 5.56-5.41 (m, 2H), 4.77-4.64 (m, 2H), 2.35-2.27 (m, 1H), 2.20-2.12 (m, 1H), 1.39-1.24 (m, 16H), 0.95-0.83 (m, 12H). $^{13}$C NMR (75 MHz, $CDCl_3$) δ 193.8, 190.8, 161.5, 137.2, 136.7, 135.6, 131.3, 131.0, 130.4, 128.1, 125.1, 124.8, 121.8, 57.5, 50.8, 37.4, 37.0, 30.7, 30.6, 28.7, 28.6, 24.1, 24.0, 23.1, 14.0, 11.0, 10.7; HRMS: calculated for $C_{30}H_{38}N_2OS_3$ + $H^+$, 539.2225; found: 523.2239 (M+)

**OTFT device fabrication and measurements**

An n-type heavily doped Si wafer with a $SiO_2$ layer of 500 nm and a capacitance of 7.5 nF $cm^{-2}$ was used as the gate electrode and dielectric layer. The thin films (40–60 nm) of S-NDI/NDI were deposited on octadecyltrichlorosilane (OTS)-treated $SiO_2$/Si substrates by spin-coating of their $CHCl_3$/hexane solutions (10 mg/mL). Next, the thin films were annealed at 60 °C, 100 °C, or 140 °C. Gold source and drain contacts (30 nm in thickness) were deposited by vacuum evaporation on the organic layer through a shadow mask, affording a bottom-gate top-contact device configuration. The channel length (*L*) and width (*W*) were 20 μm and 200 μm, respectively. Electrical measurements of OTFT devices were carried out at room temperature in air using a Keithley 4200 semiconductor parameter analyzer. The mobilities were determined in the saturation regime by using the equation $I_{DS} = (\mu WC_i/2L)(V_G - V_T)^2$, where $I_{DS}$ is the drain-source current, $\mu$ is the field-effect mobility, *W* is the channel width, *L* is the channel length, $C_i$ is the capacitance per unit area of the gate dielectric layer, and $V_T$ is the threshold voltage.

## Results and discussion

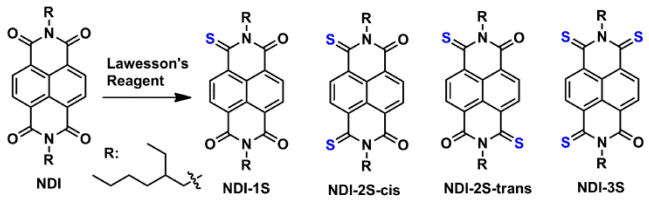


**Scheme 1** Synthetic route for the thionated NDI derivatives

The synthetic route to thionated derivatives of NDI is shown in **Scheme 1**. The parent **NDI** was synthesized according to a modified literature procedure and used as a control molecule throughout this study.[43] By varying the reaction time and the ratio between LR and **NDI**, different degree of thionation as well as different yields of the thionated derivatives can be achieved. For instance, when **NDI** was treated with 2.0 eq. of LR and heated at 140 °C for 2 h, **NDI-1S** was isolated as major product in 33% yield as well as minor product bis-thionated NDI (including **NDI-2S-trans** and **NDI-2S-cis**) in total 11% yield. No **NDI-3S** was observed. When LR was increased to 5.0 eq. with longer reaction time (24hr), no **NDI-1S** was observed, instead, **NDI-2S-trans, NDI-2S-cis** and **NDI-3S** was obtained in 11%, 9% and 4.6% yield, respectively. Although a lot of reaction conditions (temperature, ratio, reaction time) have been employed to approach **NDI-4S**, unfortunately, none of them worked. One possible reason is due to the much lower LUMO (–4.15 eV, **table 1**) of **NDI-3S**, the reactivity of LR is not strong enough to replace the fourth oxygen on **NDI-3S**.

The $^1$H NMR spectra of as-prepared **NDI-1S**, **NDI-2S-trans**, **NDI-2S-cis** and **NDI-3S** are showed as **Fig. 1**. Compared with precursor **NDI**, aromatic hydrogen atoms (**H**) on **NDI-1S** split into three groups of peaks from 8.5 to 9.0 ppm. Meanwhile, **H** on ***CH2-N*** also splits into two group peaks and one of them moves from 4.2 ppm to 4.7 ppm due to the strong electron-withdrawing property of newly-formed C=S bond. For the **NDI-2S-cis**, because the environment of **H** on the same side of aromatic ring

is the same, only two single peaks from 8.5 to 9.0 ppm are observed. As to **NDI-2S-trans**, because the environment of **H** on the same side of aromatic ring is different to each other (one is

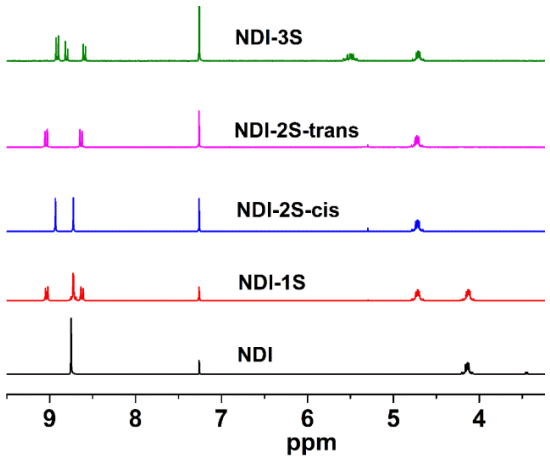


**Fig. 1** Partial $^{1}$H NMR spectra of the thionated NDI derivatives

next to C=O bond while the other is next to C=S bond), two double peaks from 8.5 to 9.0 ppm are seen. Compared with **H** on ***CH2-N*** of **NDI-2S**, the **H** on ***CH2-N*** of **NDI-3S** shift more to low field (5.5 ppm) due to the effect of the additional sulfur substitution. The structures of all compounds were further confirmed by $^{13}$C NMR, and HRMS. (Fig. S4, S5) Thermogravimetric analysis (TGA) analysis indicate that **NDI-2S-trans** is the most stable compound and decomposed at around 350 $^{o}$C while **NDI**, **NDI-1S** and **NDI-2S-cis** almost have the same decomposed temperature at ~ 325 $^{o}$C. It is worth to note that **NDI-3S** is the most unstable compound and decomposes at around 250 $^{o}$C. (**Fig. 2a**) The differential scanning calorimetry (DSC) spectra suggest that the melting peaks of these thionated derivatives are between 183 $^{o}$C and 192 $^{o}$C, which are lower than that of parent compound **NDI** (205 $^{o}$C). (**Fig. 2b**)

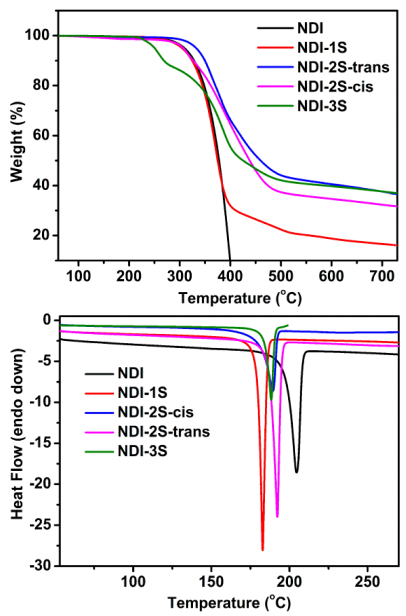


**Fig. 2a)** TGA and **2b)** DSC spectra of thionated NDI derivatives

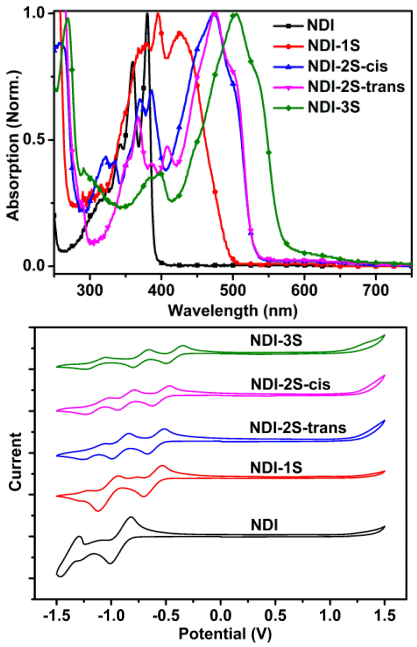


**Fig. 3a)** UV-vis absorption spectra in dried $CH_2CH_2$ and **3b**) Cyclic voltammetry (CV) of the thionated NDI derivatives

UV-vis absorption spectra of the thionated derivatives in diluted methylene chloride are displayed in **Fig. 3a**. It can be clearly seen that with successive replacement of O with S in the framework of **NDI**, the onsets of absorption of as-prepared compounds red-shift simultaneously from 400 nm to 580 nm. It's worth mentioning that although the **NDI-2S-trans** and **NDI-2S-cis** have different thionation position, their onset absorptions are almost same (530 nm). The electrochemical properties of thionated NDI as well as the parent compound **NDI** were further studied by cyclic voltammetry (CV) in 0.1 M *n*-$Bu_4NPF_6$ dry methylene chloride solution and their CV graphs are shown in **Fig. 3b**. For the control group **NDI**, the first reduction potential ($E_{1/2}$) is –0.91V vs Pt/$Pt_xO$ and it can be calculated that its onset of reduction potential ($E_{red}^{onset}$) versus $FeCp_2^{+/0}$ (+0.23 V vs Pt/$Pt_xO$, Fig. S1) was about –1.14 V. Thus, the LUMO energy was estimated to be –3.66 eV from the reduction potential by using the empirical formula, $E_{LUMO}$ = –($E_{red}^{onset}$ + 4.8) eV, assuming the absolute energy level of $FeCp_2^{+/0}$ to be 4.8 eV below vacuum.[44] The Highest Occupied Molecular Orbital (HOMO) of **NDI** is 6.86 eV calculated from LUMO and $E_g^{opt}$. Using the same method, the LUMO and HOMO values of 1S, 2S, 3S derivatives can also be obtained and the data are summarized in **Table 1**. Interestingly, in the CV graph, the **NDI-1S** has the largest shift compared with **NDI**, which corresponds with the tendency observed in UV-vis spectra (red-shift about 100 nm from **NDI** to **NDI-1S**). Thus, compared with the other strategies for LUMO level displacement,[45] thionation provides an alternative method to adjust LUMO level with concise synthesis step.

To investigate how the thionation of the parent compound **NDI** influences electron transport property over macroscopic dimensions, we fabricated and characterized thin-film field-effect transistors with bottom gate top contact configuration and gold as source/drain electrodes. Except **NDI-3S** (moderate solubility), all thionated derivatives have good solubility in common solvents

**Table 1.** Optical properties and energy levels of the thionated NDI

| | $\lambda_{onset}$ (nm) | $E_g^{opt}$ (eV)[a] | $E_{1/2}$ (V) | $E_{red}^{onset}$ (V)[b] | LUMO (eV)[c] | HOMO (eV)[d] |
|---|---|---|---|---|---|---|
| **NDI** | 388 | 3.20 | –0.91 | –1.14 | –3.66 | –6.86 |
| **NDI-1S** | 495 | 2.51 | –0.62 | –0.85 | –3.95 | –6.46 |
| **NDI-2S-trans** | 529 | 2.34 | –0.59 | –0.82 | –3.98 | –6.32 |
| **NDI-2S-cis** | 529 | 2.34 | –0.55 | –0.78 | –4.02 | –6.36 |
| **NDI-3S** | 571 | 2.17 | –0.42 | –0.65 | –4.15 | –6.32 |

[a] $E_g^{opt}$ was calculated from 1240nm/$\lambda_{onset}$. [b] $E_{red}^{onset} = (E_{1/2} - E_{1/2}(Fc/Fc^+ = +0.23))$ [c] LUMO = $-(E_{red}^{onset} + 4.8)$ eV. [d] HOMO = LUMO $-E_g^{opt}$

(e.g. chloroform, toluene), which are easy to realize solution process. Note that the solubility of thionated NDIs strongly depends on the degree of thionation: with more sulfur atoms, the solubility decreased. For a parallel comparison, chloroform/hexane has been chosen as the solvent for all devices' fabrication and the procedures are described in experimental section. Typically, S-NDI solutions were spin-coated onto OTS-treated $SiO_2$ (500 nm)/$n^{++}$Si substrates under ambient conditions. The resulted films were then subsequently annealed for about 60 min at different temperatures in a vacuum oven.

The microstructures of all as-fabricated thin-films were investigated by using atomic force microscope (AFM) and two-dimensional (2D) X-ray diffraction (XRD) techniques. As shown in Fig. S2, the substrate temperature has significant effect on the morphology and crystallinity of microstructures, which were

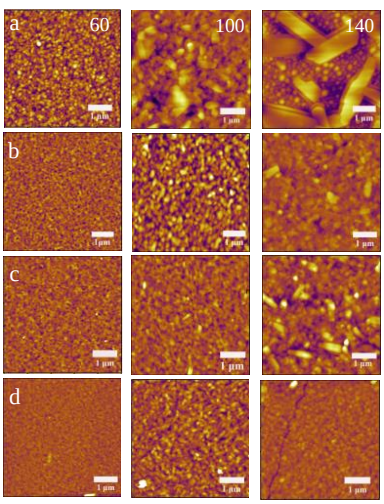


**Fig. 4** AFM images of thionated NDIs based films (a: **NDI-1S**, b: **NDI-2S-trans**, c: **NDI-2S-cis**, d: **NDI-3S**, size: 5×5 μm; annealed at 60 °C, 100 °C and 140 °C).

supposed to affect the corresponding charge transport properties of the films. Only one intense reflection peak at $2\theta = 4.85^o$ was observed for all the as-prepared films, corresponding to a d-spacing of 1.89 nm, which is close to that of the molecular lengths along the long axis (~2.30 nm, Fig. S3). Thus, the S-NDI molecules positions on the substrate with their long axes inclined at an angle of about $55^o$ onto the substrate. But at higher annealing temperature, stronger peak intensity at the same position was observed, suggesting the higher crystallinity. The

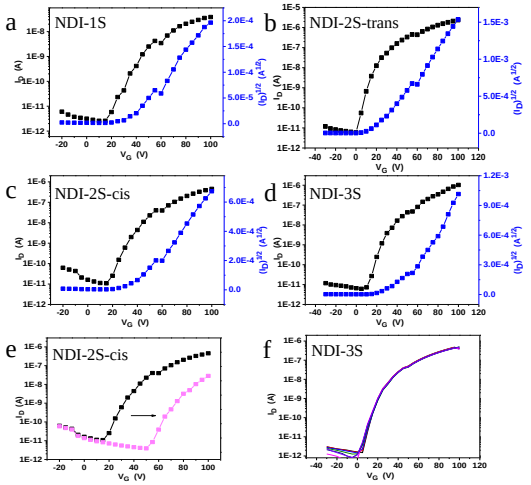


**Fig. 5**. Typical transfer characteristics of thin-film OFETs of thionated NDIs after annealing at optimized temperature for a) 140 °C, b) 140 °C, c) 140 °C, d) 100 °C and device repeatability for e, f.

**Table 2.** Detailed performance of OFETs based on thin films of thionated NDIs on OTS-treated $SiO_2$/Si substrates at various annealing temperature ($T$)

| | $T$ (°C) | $\mu$ ($cm^2\ V^{-1}\ s^{-1}$) | $I^{on}/I^{off}$ | $V_T$ (V) |
|---|---|---|---|---|
| **NDI-1S** | 60 | no field-effect | | |
| | 100 | $6.1\times10^{-5}$ | $5\times10^3$ | 27 |
| | 140 | $3.0\times10^{-4}$ | $1\times10^4$ | 28 |
| **NDI-2S-trans** | 60 | $2.4\times10^{-4}$ | $4\times10^2$ | 30 |
| | 100 | $1.7\times10^{-3}$ | $2\times10^4$ | 16 |
| | 140 | $1.0\times10^{-2}$ | $4\times10^5$ | 19 |
| **NDI-2S-cis** | 60 | $4.8\times10^{-4}$ | $1\times10^4$ | 33 |
| | 100 | $5.6\times10^{-4}$ | $4\times10^4$ | 36 |
| | 140 | $3.7\times10^{-3}$ | $4\times10^4$ | 37 |
| **NDI-3S** | 60 | $1.7\times10^{-3}$ | $4\times10^4$ | 27 |
| | 100 | $7.3\times10^{-3}$ | $2\times10^5$ | 33 |
| | 140 | $3.0\times10^{-3}$ | $4\times10^5$ | 22 |

morphology and domain sizes of as-fabricated films studied by AFM (**Fig. 4**) showed similar trends as the XRD results. When the substrate was annealed at a low temperature (60 °C), the film deposited on OTS-treated SiO2/Si substrate consisted of small grains. At a higher annealing temperature (100 °C or 140 °C), bigger grains with a more ordered film on the OTS/$SiO_2$/Si substrate were investigated. In contrast, high temperature caused NDI-3S-based films cracked large grain boundaries were observed, and the grain size stopped getting larger, which might be due to the decreased melting point.

All as-prepared S-NDI materials show typical n-type characteristics under ambient atmosphere. Mobilities calculated from saturation regime, $I_{on}/I_{off}$ ratios and threshold voltages are summarized in **Table 2**. Typical transfer curves of S-NDI-based devices are depicted in **Fig. 5a-d**. For comparison, the parent compound NDI device was prepared based on the same condition, but we did not observe obvious performance under air condition. For **NDI-1S** based devices after annealing at 60 °C,

nearly no mobility was measured, however, higher temperature annealing can increase electron mobility and the best mobility for **NDI-1S**-based devices is $3.0 \times 10^{-4}$ $cm^2$ $V^{-1}$ $s^{-1}$ at annealing temperature of 140 °C with an on/off current ratio up to $1.5 \times 10^4$. Note that the performance of the **NDI-1S** TFTs degraded on exposure to the atmosphere quickly and the repeatability of the device are very poor. Different from **NDI-1S**, **NDI-2S-trans** and **NDI-2S-cis** have higher mobilities and, with the increased annealing temperature, the mobility can be further enhanced ($\mu_{max}$ = $1.0 \times 10^{-2}$ $cm^2$ $V^{-1}$ $s^{-1}$, $4.2 \times 10^{-3}$ $cm^2$ $V^{-1}$ $s^{-1}$, with 140 °C annealing). Although **NDI-2S-trans** and **NDI-2S-cis** exhibit better stability than **NDI-1S**, their performance and repeatability at air condition are still poor (**Fig. 5e)**. For example, after several times of operation, the threshold voltage of **NDI-2S-cis** increased from 30 V to 70 V, and the field effect mobility became much lower ($8.8\times 10^{-4}$ $cm^2$ $V^{-1}$ $s^{-1}$ compared to the original mobility of $4.2 \times 10^{-3}$ $cm^2$ $V^{-1}$ $s^{-1}$). For **NDI-3S**, the best performance was obtained at 100 °C, $7.3 \times 10^{-3}$ $cm^2$ $V^{-1}$ $s^{-1}$, this value was decreased to $3.0 \times 10^{-3}$ $cm^2$ $V^{-1}$ $s^{-1}$ at temperatures higher than 100 °C. Because of its lower LUMO energy level, **NDI-3S** was supposed to be more stable and display good repeatability as the less sensitivity to oxygen and moisture. The device has been operated for about ten times and no obvious decay was observed in the I-V curves, as shown in **Fig. 5f**. The corresponding output curves of devices are shown in Fig. S6 and there is no obvious contact resistance from the output curves. All of these results demonstrated that simple sulfur-substitution could be an effective method to achieve better charge transport property.

## Conclusions

In conclusion, four novel thionated NDIs have been successfully synthesized and characterized through one step reaction from commercially available Lawesson's Reagent. Our results indicate that the sulfur-substitutions C=S bond could significantly modulate the LUMO level, band gap, absorption and electron mobility. OTFT devices based on these materials were fabricated and all measured results indicated that all compounds are typical n-type semiconductors. The best performance was observed up to 0.01 $cm^2$ $V^{-1}$ $S^{-1}$ and an on/off ratio close to $10^5$. Further research showed that **NDI-3S** displayed best repeatability with lowest LUMO level. Our research demonstrates that thionation should be a feasible way to tune the optical and electrical property of carbonyl-contained compound in the future.

## Notes and references

[a] *School of Materials Science and Engineering, Nanyang Technological University, 50 Nanyang Avenue, Singapore 639798, Singapore. Email:- qczhang@ntu.edu.sg*

[b] *Institute for Sports Research, Nanyang Technological University, 50 Nanyang Avenue, Singapore 639798, Singapore.*

[c] *The Molecular Foundry, Lawrence Berkeley National Laboratory, Berkeley, California, 94720, United States*

[d] *Division of Chemistry and Biological Chemistry, School of Physical and Mathematical Sciences, Nanyang Technological University, Singapore 637371 (Singapore)*

‡ These two authors contribute equally to this work.

† Electronic Supplementary Information (ESI) available: [details of any general characterization, XRD, NMR and MS data, etc.]. See DOI: 10.1039/b000000x/

‡ Footnotes should appear here. These might include comments relevant to but not central to the matter under discussion, limited experimental and spectral data, and crystallographic data.

### Acknowledgements

Q.Z. thanks the financial support from AcRF Tier 1 (RG 133/14)from MOE, MOE Tier 2 (ARC 20/12 and ARC 2/13), and CREATE program (Nanomaterials for Energy and Water Management) from NRF, Singapore.

1 C. Wang, H. Dong, W. Hu, Y. Liu and D. Zhu, *Chem. Rev*., 2012, **112**, 2208-2267.
2 J. Zaumseil and H. Sirringhaus, *Chem. Rev.*, 2007, **107**, 1296-1323.
3 H. Dong, X. Fu, J. Liu, Z. Wang and W. Hu, *Adv. Mater.*, 2013, **25**, 6158-6183.
4 C. Wang, J. Zhang, G. Long, N. Aratani, H. Yamada, Y. Zhao, and Q. Zhang, *Angew. Chem Int. Ed.* 2015, **54**, 6292–6296.
5 J. Zhang, C. Wang, W. Chen, J. Wu, and Q. Zhang, *RSC advances*, 2015, **5**, 25550-25554
6 S. C. Mannsfeld, B. C. Tee, R. M. Stoltenberg, C. V. Chen, S. Barman, B. V. Muir, A. N. Sokolov, C. Reese and Z. Bao, *Nat. Mater.*, 2010, **9**, 859-864.
7 G. Li, Y. Wu, J. Gao, J. Li, Y. Zhao, and Q. Zhang, *Chem. Asian J.* 2013, **8**, 1574-1578.
8 O. Knopfmacher, M. L. Hammock, A. L. Appleton, G. Schwartz, J. Mei, T. Lei, J. Pei and Z. Bao, *Nat. Comm.*, 2014, **5**, 2954.
9 C. Wang, G. Li, and Q. Zhang, *Tetrahedron Letter*, 2013, **54**, 2633-2636.
10 C. Zhang, P. Chen and W. Hu, *Chem. Soc. Rev.*, 2015. DOI**:** 10.1039/C4CS00326H
11 J. Li and Q. Zhang, *ACS Appl. Mater. Interfaces*, 2015, DOI: 10.1021/acsami.5b00113.
12 Y. J. Cheng, S. H. Yang and C. S. Hsu, *Chem. Rev.*, 2009, **109**, 5868-5923.
13 W. Chen, X. Yang, G. Long, X. Wan, Y. Chen, and Q. Zhang, *J. Mater. Chem. C*, 2015, **3**, 4698 – 4705.
14 Q. Zhang, J. Xiao, Z. Y. Yin, H. M. Duong, F. Qiao, F. Boey, X. Hu, H. Zhang, and F. Wudl, *Chem. Asian. J.* 2011, **6**, 856-862
15 Q. Meng and W. P. Hu, *Phys. Chem. Chem. Phys.*, 2012, **14**, 14152-14164.
16 H. Usta, A. Facchetti and T. J. Marks, *Acc. Chem. Res.*, 2011, **44**, 501-510
17 B. J. Jung, N. J. Tremblay, M. L. Yeh and H. E. Katz, *Chem. Mater.*, 2011, **23**, 568-582.
18 Y. Zhao, Y. Guo and Y. Liu, *Adv. Mater.*, 2013, **25**, 5372-5391.
19 B. A. Jones, A. Facchetti, T. J. Marks and M. R. Wasielewski, *Chem. Mater.*, 2007, **19**, 2703-2705.
20 J. H. Oh, S. L. Suraru, W. Y. Lee, M. Konemann, H. W. Hoffken, C. Roger, R. Schmidt, Y. Chung, W. C. Chen, F. Wurthner and Z. N. Bao, *Adv. Funct. Mater.*, 2010, **20**, 2148-2156.
21 H. E. Katz, J. Johnson, A. J. Lovinger and W. J. Li, *J. Am. Chem. Soc.*, 2000, **122**, 7787-7792.
22 H. E. Katz, A. J. Lovinger, J. Johnson, C. Kloc, T. Siegrist, W. Li, Y. Y. Lin and A. Dodabalapur, *Nature*, 2000, **404**, 478-481.
23 L. Hao, C. Xiao, J. Zhang, W. Jiang, W. Xu and Z. Wang, *J. Mater. Chem. C*, 2013, **1**, 7812.
24 A. Lv, S. R. Puniredd, J. Zhang, Z. Li, H. Zhu, W. Jiang, H. Dong, Y. He, L. Jiang, Y. Li, W. Pisula, Q. Meng, W. Hu and Z. Wang, *Adv. Mater.*, 2012, **24**, 2626-2630.
25 W. Yue, A. Lv, J. Gao, W. Jiang, L. Hao, C. Li, Y. Li, L. E. Polander, S. Barlow, W. Hu, S. Di Motta, F. Negri, S. R. Marder and Z. Wang, *J. Am. Chem. Soc.*, 2012, **134**, 5770-5773.
26 X. Gao, C.-A. Di, Y. Hu, X. Yang, H. Fan, F. Zhang, Y. Liu, H. Li and D. Zhu, *J. Am. Chem. Soc.*, 2010, **132**, 3697-3699.
27 B. A. Jones, M. J. Ahrens, M. H. Yoon, A. Facchetti, T. J. Marks and M. R. Wasielewski, *Angew. Chem. Int. Edit*, 2004, **43**, 6363-6366.

28 A. F. Lv, S. R. Puniredd, J. H. Zhang, Z. B. Li, H. F. Zhu, W. Jiang, H. L. Dong, Y. D. He, L. Jiang, Y. Li, W. Pisula, Q. Meng, W. P. Hu and Z. H. Wang, *Adv. Mater.*, 2012, **24**, 2626-2630.

29 J. Casado, R. P. Ortiz and J. T. L. Navarrete, *Chem. Soc. Rev.*, 2012, **41**, 5672-5686.

30 Q. H. Wu, S. D. Ren, M. Wang, X. L. Qiao, H. X. Li, X. K. Gao, X. D. Yang and D. B. Zhu, *Adv. Funct. Mater.*, 2013, **23**, 2277-2284.

31 Y. Suzuki, E. Miyazaki and K. Takimiya, *J. Am. Chem. Soc.*, 2010, **132**, 10453-10466.

32 Y. L. Qiao, Y. L. Guo, C. M. Yu, F. J. Zhang, W. Xu, Y. Q. Liu and D. B. Zhu, *J. Am. Chem. Soc.*, 2012, **134**, 4084-4087.

33 W. Yue, T. He, M. Stolte, M. Gsanger and F. Wurthner, *Chem. Commun.*, 2014, **50**, 545-547.

34 R. R. Dasari, A. Dindar, C. K. Lo, C. Y. Wang, C. Quinton, S. Singh, S. Barlow, C. Fuentes-Hernandez, J. R. Reynolds, B. Kippelen and S. R. Marder, *Phys. Chem. Chem. Phys.*, 2014, **16**, 19345-19350.

35 R. C. Haddon, *J. Am. Chem. Soc.*, 1996, **118**, 3041-3042.

36 M. Kitamura, S. Aomori, J. H. Na and Y. Arakawa, *Appl. Phys. Lett.*, 2008, **93**, 033313.

37 J. N. Haddock, X. Zhang, B. Domercq and B. Kippelen, *Org. Electron.*, 2005, **6**, 182-187.

38 R. Rodel, F. Letzkus, T. Zaki, J. N. Burghartz, U. Kraft, U. Zschieschang, K. Kern and H. Klauk, *Appl. Phys. Lett.*, 2013, **102**.

39 T. Okamoto, C. Mitsui, M. Yamagishi, K. Nakahara, J. Soeda, Y. Hirose, K. Miwa, H. Sato, A. Yamano, T. Matsushita, T. Uemura and J. Takeya, *Adv. Mater.*, 2013, **25**, 6392-6397.

40 I. McCulloch, M. Heeney, C. Bailey, K. Genevicius, I. Macdonald, M. Shkunov, D. Sparrowe, S. Tierney, R. Wagner, W. Zhang, M. L. Chabinyc, R. J. Kline, M. D. McGehee and M. F. Toney, *Nat. Mater.*, 2006, **5**, 328-333.

41 A. Kim, K. S. Jang, J. Kim, J. C. Won, M. H. Yi, H. Kim, D. K. Yoon, T. J. Shin, M. H. Lee, J. W. Ka and Y. H. Kim, *Adv. Mater.*, 2013, **25**, 6219-6225.

42 Y. Yuan, G. Giri, A. L. Ayzner, A. P. Zoombelt, S. C. Mannsfeld, J. Chen, D. Nordlund, M. F. Toney, J. Huang and Z. Bao, *Nat. Commun.*, 2014, **5**, 3005.

43 C. Thalacker, C. Roger and F. Wurthner, *J. Org. Chem.*, 2006, **71**, 8098-8105.

44 J. Pommerehne, H. Vestweber, W. Guss, R. F. Mahrt, H. Bassler, M. Porsch and J. Daub, *Adv. Mater.*, 1995, **7**, 551.

45 F. Wurthner and M. Stolte, *Chem. Commun.*, 2011, **47**, 5109–5115.

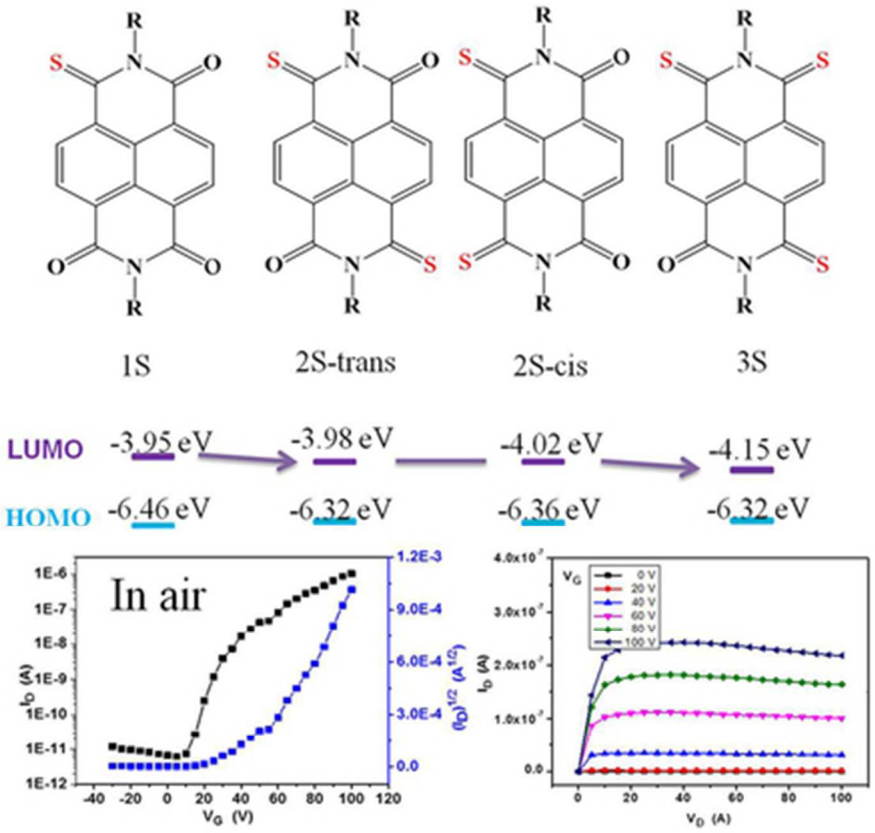


39x35mm (300 x 300 DPI)

We demonstrated that the electron mobility of naphthalene diimide (NDI) in thin film transistors (TFTs) under ambient conditions can be dramatically enhanced through a simple step reaction by replacing oxygen atoms with sulfur atoms.